Anti-tau monoclonal antibodies derived from soluble and filamentous tau show diverse functional properties in vitro and in vivo

Journal of Alzheimer's Disease xx (20xx) x–xx
DOI 10.3233/JAD-180404
IOS Press

Anti-Tau Monoclonal Antibodies Derived from Soluble and Filamentous Tau Show Diverse Functional Properties *in vitro* and *in vivo*

Marc Vandermeeren[a,1], Marianne Borgers[a,1], Kristof Van Kolen[a,*], Clara Theunis[a], Bruno Vasconcelos[a], Astrid Bottelbergs[a], Cindy Wintmolders[a], Guy Daneels[a], Roland Willems[a], Koen Dockx[b], Lore Delbroek[a], André Marreiro[a], Luc Ver Donck[a], Cristiano Sousa[a], Rupesh Nanjunda[c], Eilyn Lacy[c], Tom Van De Casteele[d], Debby Van Dam[e,f], Peter Paul De Deyn[e,f,g,h], John Kemp[a], Thomas J. Malia[c] and Marc H. Mercken[a]

[a]*Neuroscience Department, Janssen Research and Development, Beerse, Belgium*
[b]*Discovery Sciences, Janssen Research and Development, Beerse, Belgium*
[c]*Biologics Research, Janssen Research and Development, Spring House, PA, USA*
[d]*Non-Clinical Statistics, Janssen Research and Development, Beerse, Belgium*
[e]*Laboratory of Neurochemistry and Behavior, Institute Born-Bunge, University of Antwerp, Antwerp, Belgium*
[f]*Department of Neurology and Alzheimer Research Center, University Medical Center Groningen (UMCG), Groningen, The Netherlands*
[g]*Department of Neurology and Memory Clinic, Hospital Network Antwerp (ZNA) Middelheim and Hoge Beuken, Antwerp, Belgium*
[h]*Biobank, Institute Born-Bunge, University of Antwerp, Antwerp, Belgium*

Accepted 21 June 2018

Abstract. The tau spreading hypothesis provides rationale for passive immunization with an anti-tau monoclonal antibody to block seeding by extracellular tau aggregates as a disease-modifying strategy for the treatment of Alzheimer's disease (AD) and potentially other tauopathies. As the biochemical and biophysical properties of the tau species responsible for the spatio-temporal sequences of seeding events are poorly defined, it is not yet clear which epitope is preferred for obtaining optimal therapeutic efficacy. Our internal tau antibody collection has been generated by immunizations with different tau species: aggregated- and non-aggregated tau and human postmortem AD brain-derived tau fibrils. In this communication, we describe and characterize a set of these anti-tau antibodies for their biochemical and biophysical properties, including binding, tissue staining by immunohistochemistry, and epitope. The antibodies bound to different domains of the tau protein and some were demonstrated to be isoform-selective (PT18 and hTau56) or phospho-selective (PT84). Evaluation of the antibodies in cellular- and *in vivo* seeding assays revealed clear differences in maximal efficacy. Limited proteolysis experiments support the hypothesis that some epitopes are more exposed than others in the tau seeds. Moreover, antibody efficacy seems to depend on the structural properties of fibrils purified from tau Tg mice- and postmortem human AD brain.

Keywords: Epitope mapping, immunotherapy, *in vivo* seeding, tau antibodies

[1]These authors contributed equally to this work.

*Correspondence to: Kristof Van Kolen, Neuroscience Department, Janssen Research and Development, 2340 Beerse, Belgium. E-mail: kvkolen@its.jnj.com.

INTRODUCTION

Despite the large heterogeneity in neurodegenerative diseases, protein misfolding and aggregation seems to be a common underlying mechanism leading to neuronal dysfunction [1]. The presence of tau inclusions in Alzheimer's disease (AD) justifies classifying it as a tauopathy [2]. Although in AD both amyloid and tau pathology are critical, it is important to refer that in certain tauopathies such as frontotemporal lobar degeneration with tau inclusions (FTLD-tau), Pick's disease, progressive supranuclear palsy, corticobasal degeneration, and argyrophilic grain disease, amyloid pathology is not prominent, indicating that tau dysfunction on its own may be toxic [3].

Tau protein is codified by a single gene, *MAPT*, located on locus 17q21.3 comprising 16 exons of which three (exon 2, 3 (coding for N-terminal inserts (N) and exon 10 coding for an additional repeat (R) domain) are targets of alternative splicing resulting in six isoforms (0N3R, 0N4R, 1N3R, 1N4R, 2N3R, 2N4R) [3]. Tau is abundantly expressed in the central nervous system, especially in neurons [4]. Its function in microtubule stabilization suggests that disruption of microtubules, which are critical to axonal structure and transport, may be one way by which aberrant tau leads to neurodegeneration [5]. However, pathological tau is hyperphosphorylated and aggregates into insoluble neurofibrillary tangles (NFTs) via a series of conformational changes. Therefore, tau-mediated toxicity is believed to be exerted by accumulation of intracellular aggregates or intermediate products of those aggregates [6–8].

In the context of AD, NFTs propagate in a hierarchical and predictable pattern through selective brain regions and the degree of NFT deposits is used to define disease progression in different pathological "Braak" stages [9]. An extensive study showing the immunohistochemical (IHC) (and histochemical) analysis of a large (non-selected) set of postmortem human brain samples showed AT8-positive signals (pre-tangles) in sections from individuals younger than 30 years old [10]. Over time, pathology spreads from the locus coeruleus toward cortical regions via transenthorinal- and subcortical regions [11]. Although the pattern of propagation and the brain regions affected by tau pathology have been identified, it is not completely understood how this mechanism of spreading occurs. Initially, the spread of tau pathology in AD was attributed to the passive release of tau from neurons due to cell death. However, recently, several research groups demonstrated active release and interneuronal transfer of tau, suggesting a trans-neuronal spread of misfolded tau [12–14]. To date, the most advanced therapeutic strategies to block tau spreading in humans, involve active tau immunization or passive immunization with anti-tau monoclonal antibodies. Several studies have shown beneficial effects of both immunization approaches in transgenic mouse models of tauopathy [15–17] but it is not clear which epitope in tau is most suited to target seeding. Recent research demonstrated efficient seeding by tau fibrils isolated from tau transgenic mice (expressing the 0N4R isoform of human tau with a P301S mutation) or from postmortem human tauopathy brain [18–20] suggesting that human paired-helical filaments (PHFs) are relevant antigens for immunization to develop antibodies for research and therapeutic purposes. Here we report on the development and characterization of tau antibodies obtained by immunizing tau knockout (KO) mice with monomeric tau, recombinant tau aggregates and filamentous tau isolated from human AD brain.

MATERIALS AND METHODS

All *in vivo* experiments were conducted in strict accordance with to the guidelines of the Association for Assessment and Accreditation of Laboratory Animal Care International (AAALAC), with the European Communities Council Directive of 24 November 1986 (86/609/EEC) and with protocols approved by the local Institutional Animal and Use Ethical Committee.

Preparation of postmortem human AD brain-derived PHFs

PHF-tau for immunizations was kindly provided by Drs. Wencheng Liu and Steven Paul (Weill Medical College of Cornell University, New York, USA). Postmortem tissue from the cortex obtained from a histologically confirmed AD patient (Braak stage VI) was partially purified by a modified method of [21]. Typically, 5 g of frontal cortex was homogenized in 10 volumes of cold buffer H (10 mM Tris, 800 mM NaCl, 1 mM EGTA and 10% sucrose/ pH 7.4) using a glass/Teflon Potter tissue homogenizer (IKA Works, Inc; Staufen, Germany) at 1000 rpm. The homogenized material was centrifuged at 27000× *g* for 20 min. The pellet was discarded and the supernatant was adjusted to a final concentration of 1% (w/v)

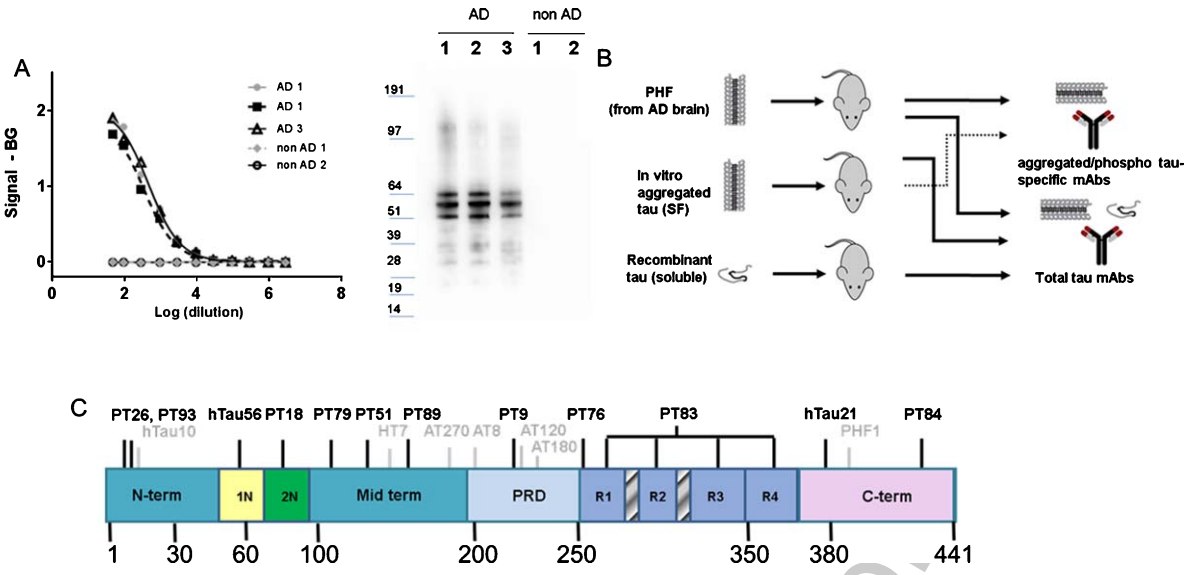

Fig. 1. A) Representative characterization of PHFs derived from postmortem human AD brain (and preps from non-AD controls) with aggregation-selective ELISA and western blot (AT8). The latter shows a typical profile of the six hyperphosphorylated (full length) tau isoforms running as a triplet between 55 and 65 kDa. B) Overview of tau immunizations with different types of antigens resulting in PHF/phospho tau selective antibodies (PT84) and antibodies reacting with both PHF and recombinant tau. C) Epitope position mapped against the longest human tau isoform (2N4R) encompassing amino terminus (N-term), N-terminal inserts (1N and 2N), mid-term, proline-rich domain (PRD), microtubule-binding domain (MTBD) which consists of 4 repeats R1-R4 in 4R isoforms and 3 repeats (R1, R3, R4) in 3R isoforms and the carboxy-terminus (C-term) of the tau antibodies discussed in this manuscript (new antibodies in black; reference antibodies in gray).

N-lauroylsarcosine and 1% (v/v) 2-mercaptoethanol and incubated for 2 h at 37°C. Subsequently the supernatant was centrifuged at 184000× *g* for 90 min at 20°C. The pellet was carefully washed in PBS and resuspended in 750 μL PBS, aliquoted and frozen at –80°C. The quality of the PHF-tau preparations was evaluated by the use of AT8/AT8 phospho-aggregate-selective ELISA and by western blotting with the anti phospho tau antibody AT8 (pS202/pT205/pS208) [22] (Janssen R&D) (Fig. 1A). Total protein which is detected by ECL Plex Goat-anti-Mouse IgG-Cy3 from Amersham (PA43009) (Supplementary Figure 1A).

Immunization of mice and fusion

Immunizations in Tau KO mice (The Jackson Laboratory, Bar Harbor, ME, USA) with PHFs or recombinant 2N4R (P301S) tau (Tebu Bio, Le Perray-en-Yvelines, France) aggregated *in vitro* as described in [23], were performed using standard hybridoma technology [24].

Briefly, female tau KO mice were immunized with 100 μg of *in vitro* aggregated P301S tau or 50 μg of human PHF tau for each immunization. Before intraperitoneal injection, antigen was mixed with complete or incomplete Freund's adjuvant (Millipore Sigma, St. Louis, MO, USA). Mice were boosted every two weeks with aggregated tau preparation, first in complete and subsequently in incomplete Freund's adjuvant. Four days before spleen extraction, mice were boosted with aggregated tau prep in saline. Following this immunization regime, spleen cells were harvested and fused with myeloma cells to generate hybridomas.

Obtained hybridomas were seeded in 96-well plates and screened after 10 days in a direct ELISA on 25 ng/well coated PHF-tau. Positive cells were tested for cross-reactivity with soluble tau on ELISA plates coated with 10 ng/well recombinant 2N4R tau and were immediately subcloned and frozen in liquid nitrogen. All hybridomas were grown in Dulbecco's modified Eagle's medium supplemented with 10% fetal calf serum (Hyclone, Europe), Hybridoma Fusion Cloning Supplement (2%) (Roche Diagnostics, Mannheim, Germany), 2% HT (Millipore Sigma), 1 mM sodium pyruvate, 2 mM L-glutamine and penicillin (100 U/ml), and streptomycin (50 mg/ml). Antibody variable regions were cloned from selected hybridoma cells, sequenced using standard methods, and subcloned into expression vectors for mAb and Fab. Mab was produced on a mouse

IgG2a/κ background and expressed and purified by affinity chromatography (protein A). Fab was produced as chimeric versions with the mouse variable domains fused to human IgG1/κ constant domains and a His tag at the C-terminus of the heavy chain. Fab was transiently expressed in HEK293F cells and purified by affinity chromatography (HisTrap).

Surface plasmon resonance (SPR)

The interaction of anti-tau mAbs with PHF-tau was analyzed by ProteOn (BioRad, Hercules, CA, USA) as described before [22]. The interaction of anti-tau Fabs or mAbs with recombinantly expressed control tau (human tau isoform 2N4R) was studied with a Biacore T200 (GE Healthcare, Marlborough, MA, USA). A biosensor surface was prepared by coupling an anti-mouse IgG Fc- or Fab-domain specific antibody to the surface of a CM5 sensor chip using the manufacturer's instructions for amine-coupling chemistry (~6500 RU). The coupling buffer was 10 mM sodium acetate, pH 4.5. The anti-tau Fabs or mAbs were diluted in the running buffer and injected to obtain a capture of at least 5 RU. Capture of anti-tau mAbs or Fabs was followed by injection of recombinantly expressed control tau in solution (0.12 to 75 nM in 5-fold dilutions). The association was monitored for 3 min (150 µL injected at 50 µL/min). The dissociation was monitored until the signal decreased by at least 5% for reasonable off-rate determination. Regeneration of the sensor surface was obtained with 0.85% phosphoric acid followed by 50 mM NaOH. The data for both mAbs and Fabs were fit using a 1:1 Langmuir binding model if binding was observed.

Epitope mapping

To reconstruct epitopes of the target molecule a library of peptides (20-mers with an overlap of 18 amino acids) covering the Tau 441 sequence was done using Pepscan's proprietary Chemically Linked Peptides on Scaffolds (CLIPS) technology (Pepscan Presto B.V., Lelystad, the Netherlands) [25]. The binding of antibodies (recombinantly expressed as IgG2a) to each of the synthesized peptides was tested in a Pepscan-based ELISA. The peptide arrays were incubated with primary antibody solution (overnight at 4°C). After washing, the peptide arrays were incubated with a 1/1000 dilution of a peroxidase conjugated anti mouse antibody for 1 h at 25°C. After washing, the peroxidase substrate 2,2'-azino-di-3-ethylbenzthiazoline sulfonate (ABTS) and 20 µl/mL of 3% H_2O_2 were added. After 1 h, the color development was quantified with a charge coupled device (CCD)-camera and an image processing system.

Sarcosyl extraction from mouse brain

Tissue was weighed and homogenized in 6 volumes of buffer H (10 mM Tris, 800 mM NaCl, 1 mM EGTA and 10% sucrose/ pH 7.4). The homogenate was centrifuged at 27 000× *g* for 20 min and 1% N-lauroylsarcosine was added to the supernatant. After 90 min, the solutions were again centrifuged at 184 000× *g* for 1 h. The supernatants were kept as sarkosyl-soluble fraction, whereas the pellet containing the sarkosyl-insoluble material was resuspended in homogenization buffer.

Direct ELISA

Nunc MaxiSorp™ high protein-binding capacity 96 well ELISA plates were coated either with ePHF or with sarkosyl insoluble fraction from spinal cord of 22 to 23 weeks-old P301S transgenic animals, diluted in coating buffer (10 mM Tris, 10 mM NaCl pH 8.5; 50 µL per well) and left overnight at 4°C. The plate was washed 5 times with PBS-T and overcoated with 75 µL of blocking solution (0.1% Casein in PBS) per well and left for at least 1 h at room temperature. After blocking, the plate was washed again. Different concentrations of primary antibodies were diluted in blocking solution and 50 µL was added to the assay plate, with an overnight incubation at 4°C. After incubation with sample, plates were again washed and 50 µL per well of Goat Anti-Mouse IgG (H L)-HRP Conjugate (BioRad) diluted 1:2500 in blocking buffer was added. Another wash was made and detection was performed with TMB Peroxidase EIA Substrate kit (BioRad) according to the manufacturers' instructions. After 5 min, an equal volume of 2N H_2SO_4 was added to stop the enzymatic reaction. Detection was performed in Perkin Elmer EnVision® 2102 Multilabel Reader at OD_{450nm}. Binding curves were generated using GraphPad Prism7.0 software.

Western blotting

Brain tissue from wild type (WT: C57Bl/6J) and Tau KO mice, beagle dog, and cynomolgus monkey were obtained according to procedures approved by the local ethical committee and national institutions

adhering to AAALAC guidelines. Human brain tissue was obtained from the IBB Biobank. For total homogenates, tissue was weighed and homogenized in 6 volumes of buffer H (10 mM Tris, 800 mM NaCl, 1 mM EGTA, and 10% sucrose/ pH 7.4). The homogenate was centrifuged at 27000× *g* for 20 min and the supernatant was aliquoted and frozen at –80°C. To prepare heat-stable extract (HSE), homogenate is boiled for 5 min (100°C) and cooled on ice for 10 min. After ultracentrifugation (150000× *g*; 4°C; 2 h) supernatants containing HSE are aliquoted and frozen at –80°C. Samples were diluted in sample buffer and loaded on SDS (4–12%) or native (3–12%) PAGE (Life Technologies, Thermo Scientific) according to the manufacturer's instructions. After the separation, the gel was blotted on a nitrocellulose membrane which was blocked with TBS-T containing 5% non-fat dry milk. Blots were incubated with non-labelled primary antibody solutions (overnight at 4°C) and detected by HRP-labelled anti mouse antibodies. Incubation with HRP-labelled tau antibodies was performed during 2 h at RT. In both cases detection was done with West Dura (Thermo Scientific).

Immunohistochemistry (IHC)

Brains of sacrificed mice were removed from the skull and fixed overnight in a formalin-based fixative, followed by paraffin embedding and sectioning of 5 μm thick sagittal sections. After deparaffinization, rehydration, quenching of endogenous peroxidase, and heat-induced epitope retrieval in citrate buffer (pH 6), primary antibody (1 μg/mL) was applied to the sections for 1 h. Extensive rinsing was followed by 30 min incubation with anti-mouse secondary antibody (Envision, DAKO, Glostrup, Denmark) and chromogenic labelling using 3,3-diaminobenzidine (DAKO). Following hematoxylin counterstaining, sections were dehydrated and mounted. For double-labelling experiments, primary antibodies AT8(IgG2a) and PT84(IgG1) were visualized with Alexa488 labelled anti-mouse IgG2a and Alexa555 labelled anti-mouse IgG1 (Life Technologies, Thermo Scientific). Sections were imaged with the Hamamatsu NanoZoomer slidescanner (Hamamatsu Photonics, Shizuoka, Japan).

Cryopreserved human brain tissue was sliced with a cryostat (20 μm thickness) and stored at –80°C before use. Sections were dried, followed by formalin fixation, blocking of endogenous peroxidase with 3% hydrogen peroxide (DAKO, Glostrup, Denmark, S2023) and permeabilization in PBS1x + 0.3% Triton X-100 during 1 h. Primary antibodies (0.4 μg/ml) were diluted in antibody diluent with background reducing components (DAKO, S3022) and applied to the sections for 1 h. After extensive washing, slides were incubated with HRP-conjugated anti-mouse secondary antibody (Envision, DAKO, K4000), followed by chromogenic DAB labelling (DAKO, K4368). Slides were counterstained with hematoxylin, dehydrated and mounted with organic mounting medium (Vectamount, Vector labs, Burlingame, CA, USA, H-5000). Imaging was performed with a Hamamatsu NanoZoomer 2.0 rs (Hamamatsu Photonics, Shizuoka, Japan).

Cell-based assays

In the immunodepletion assays, tau seeds were incubated with test antibody and removed from the solution with protein G-coupled magnetic beads (Life Technologies, Thermo Scientific). In addition to a number of our internal tau antibodies, the following reference tau antibodies (Fig. 1C) were included for comparison (unless specified otherwise, antibodies were purified in house): hTau10 (29–36) [23], HT7 (159–164) (Thermo Scientific), AT120 [26] (217–224), AT8 (pS202/pT205/pS208) [22], AT180 (pT231), AT270 (pT181) [27]. PHF1 (pS396) was a kind gift from Peter Davies (Albert Einstein College of Medicine, NY, USA). The depleted supernatant was tested for residual seeding capacity in the chromophore-K18-containing HEK cells and analyzed by FACS as previously described [28]. Homogenates containing tau seeds for immunodepletion were generated from spinal cords of 22- to 23-week-old P301S transgenic animals [29] or from cryopreserved human AD brain tissue obtained from the IBB Biobank. After depletion, the human AD supernatant was tested in the presence of the transfection reagent Lipofectamine2000 (Life Technologies, Thermo Scientific). Immunodepleted fractions from P301S spinal cord extracts are added to the cells without transfection.

Animals and stereotactic injections

For injection studies, transgenic Tau-P301L mice, expressing the longest human tau isoform with the P301L mutation (tau-4R/2N-P301L) [30], were used for surgery at the age of 3 months. All experiments were performed in compliance with protocols

approved by the local ethical committee and national institutions adhering to AAALAC guidelines. For stereotactic surgery, the mice received a unilateral (right hemisphere) injection of AD-derived PHFs in the hippocampus. Two months after injection, tissue from the *contralateral* hemisphere was analyzed with immunohistochemical staining using AT8 (Fig. 6A) while the *ipsilateral* hemisphere was processed to extract total and sarcosyl insoluble fractions as described above.

Biochemical analysis MesoScale Discovery (MSD)

Coating antibody (AT8) was diluted in PBS (1 μg/mL) and aliquoted into MSD plates (30 μL per well) (L15XA, MSD, Rockville, MD, USA), which were incubated overnight at 4°C. After washing with 5 × 200 μL of PBS/0.5%Tween-20, the plates were blocked with 0.1% casein in PBS and washed again with 5 × 200 μl of PBS/0.5% Tween-20. After adding samples and standards (both diluted in 0.1% casein in PBS), the plates were incubated overnight at 4°C. Subsequently, the plates were washed with 5 × 200 μL of PBS/0.5% Tween-20, and SULFO-TAG™ conjugated detection antibody (AT8) in 0.1% casein in PBS was added and incubated for 2 h at room temperature while shaking at 600 rpm. After a final wash (5 × 200 μL of PBS/0.5%Tween-20), 150 μL of 2 × buffer T (MSD) was added, and plates were read with an MSD imager. Raw signals were normalized against a standard curve consisting of 16 dilutions of a sarcosyl-insoluble prep from postmortem AD brain (ePHF) and were expressed as arbitrary units (AU) ePHF. Statistical analysis (ANOVA with Bonferroni post test) was performed with the GraphPad prism software and with an 'in house' developed application for automated analysis.

Limited proteolysis of tau seeds

Limited proteolysis analysis of human ePHF samples and mouse sarkosyl insoluble fractions was performed as previously described with minor modifications [31]. Briefly, after protein quantification using the BCA method, 0.85 μg/μL of the different samples were incubated with 0, 5, and 25 μg/mL of Pronase (Roche; 10165921001). The digestion reactions were performed during 1 h at 37°C, before quenching with LDS sample buffer 1X (Life Technologies) and boiling for 5 min at 95°C. Quenched samples were then added (30 μL) to a 4–20% Criterion TGX stain-free gel (Bio-Rad) and blotted onto a nitrocellulose membrane (Bio-Rad). Blocking was performed during 1 h with TBS-T containing 5% non-fat dry milk, before probing with HRPO labeled Tau specific antibodies for 2 h at room temperature. Blots were then detected with West Dura (Thermo Scientific) and image acquisition was performed in an Amersham Imager 600 (GE Healthcare Life Sciences).

RESULTS

Immunizations and selection of hybridoma clones

As tau fibrils derived from different origins have different structural properties, we performed immunizations with non-aggregated and *in vitro* aggregated recombinant tau on one hand and human-derived PHFs on the other hand. Human AD brain-derived PHF were characterized by aggregation selective ELISAs and western blotting. A representative example of this analysis and an overview of the different immunizations is shown in (Fig. 1A, B). After each fusion, hybridomas were selected based on the reactivity of their supernatants toward PHF/soluble tau on ELISA (data not shown). Supernatants from positive hybridoma clones were further tested in a western blot screen using PHF from human AD brain and another screen to heat-stable extract from human non-AD brain as antigen as described in the materials and methods section (data not shown). To obtain a diverse panel of antibodies (Fig. 1C), both PHF selective and non-selective hybridomas were selected and subcloned further. With exception of hTau21, PT18, PT84, and hTau56, variable regions of heavy- (V_H) and light chain (V_L) of all these antibodies were cloned to allow recombinant expression.

Binding properties and epitope mapping

To evaluate binding properties, surface plasmon resonance (SPR) measurements were performed to measure the interaction between tau mAbs and postmortem human AD brain-derived PHFs (Fig. 2). Intrinsic binding properties were determined by antigen binding fragment (Fab) binding on human recombinant 2N4R Tau. Compilation of the SPR data is represented in Table 1. Fab binding data are not available for hTau21, PT18, PT84, and hTau56 as V-region cloning of these has not been performed. Therefore, hybridoma-produced monoclonal antibodies (mAbs) were used for binding analysis

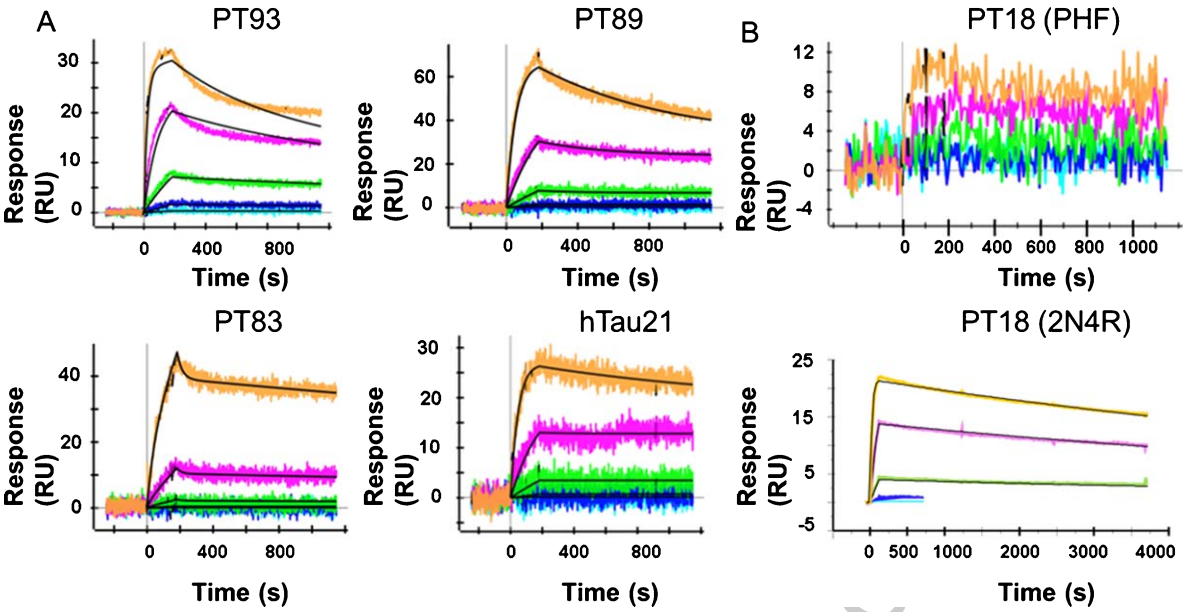

Fig. 2. Affinity of tau mAbs to PHF and soluble tau was determined by SPR. A) Representative sensorgrams of at least two independent experiments of a selection of tau mAbs to PHF is shown. B) Comparative sensorgrams of PT18 binding to PHF and 2N4R tau clearly show that its epitope has low abundance PHF. Different colors reflect the concentration of injected antibody (orange: 75 nM; pink: 15 nM; green: 3 nM; dark blue: 0.6 nM and cyan: 0.12 nM).

Table 1
Properties of different Tau mAbs generated by immunizations with human AD PHFs and recombinant Tau (aggregated or non-aggregated)

Antibody	Epitope	Immunogen	mAb Affinity PHF (nM)	Fab Affinity soluble Tau (nM)	Species reactivity
PT26	$_{23}$RKDQ$_{26}$	PHF	3.942	18.0	m, h
PT93	$_{27}$YTMHQD$_{32}$	PHF	3.389	17.1	d, m, h
hTau56	$_{57}$EEPGSE$_{62}$ (selective for 1N and 2N isoforms)	Agg. Rec human Tau	Low binding*	Low binding*	(ms), d, m, h
PT18	$_{71}$TAEDVTAP$_{78}$ (selective for 2N isoforms)	PHF	Low binding*	0.85*	ms, d, m, h
PT89	$_{173}$AKTPPA$_{178}$	PHF	3.039	Poor binding	ms, d, m, h
PT51	$_{153}$TPRGAA$_{158}$	PHF	1.216	23.3	ms, d, m, h
PT79	$_{131}$(SK)DGTGSDDKK$_{140}$	PHF	2.093	17.4	m, h
mTau5	$_{120}$DRTGNDEKKA$_{129}$ preference for mouse Tau	Rec mouse Tau	N/A	N/A	ms, (d, m, h)
PT9	$_{163}$NATRIPAK$_{174}$ + $_{219}$PTREPK$_{226}$	PHF	3.770	Poor binding	ms, d, m, h
AT120	$_{219}$PTREPK$_{226}$	PHF**	1.6	40.2	ms, d, m, h
PT76	$_{249}$PMPDLKNVKS$_{258}$	PHF	2.893	22.2	(d), m, h
PT83	$_{267}$KHQPGG$_{277}$ + $_{299}$HVPG$_{302}$ + $_{329}$HHKPGG$_{334}$ + $_{361}$THVPGG$_{366}$	PHF	8.840 (slow kon)	164.6	ms, d, m, h
PT84	$_{405}$PRHLpSN$_{410}$	PHF	1.202*	Poor binding*	
hTau21	$_{375}$KLTRFE$_{380}$	Rec human Tau	1.640*	82.8* (mAb)	ms, d, m, h

Epitopes have been determined by linear epitope mapping Pepscan® as described in materials and methods. Also, the epitope of mTau5 has been determined on a mouse peptide array. Binding properties of recombinantly produced mAbs (to PHF) and Fabs (to 2N4R Tau) was determined by SPR and are averages of at least two independent experiments. *The hTau21, hTau56, PT18, and PT84 antibodies have not been cloned and were tested as recombinant mAb. **AT120 has not been generated in this study but has been described earlier [26]. Western blot reactivity to tau from different species (ms, mouse; d, dog; m, monkey; h, human) is indicated.

to PHFs and 2N4R Tau. In comparison to the other antibodies, these mAbs displayed relatively low maximal binding signals to PHFs (almost no measurable response units (RU) for PT18). On the other hand, PT18 (0.85 nM) showed good binding to 2N4R tau (Table 1). For the other Tau mAbs (except PT9) analyzed, good binding was observed for both PHFs (Fig. 2) and soluble tau, so the differential binding

to PHFs and soluble tau by PT18 (Fig. 2B) was somewhat surprising. In the next step of the characterization process, detailed epitope mapping was performed by using a linear peptide array (20-mers with an 18-amino acid overlap) encompassing the human 2N4R tau isoform. Detailed mapping is shown for PT84 and hTau21 (Supplementary Figure 2) and all results are summarized in Table 1, demonstrating that varying epitope domains (amino (N)-terminal, mid-term, proline-rich domain (PRD), microtubule-binding domain (MTBD) and carboxy (C)-terminal) are represented in our antibody collection.

In the group of N-terminal antibodies, hTau56 and PT18 were shown to have their binding epitope in the 1N and 2N insert, respectively, which shows that both antibodies are tau isoform selective. This could potentially explain the lower binding of both antibodies to PHFs, which is presumably composed of the 6 Tau isoforms [32, 33] (Supplementary Figure 2C) from which only two contain the 2N domain and four the 1N domain.

The PRD-binding antibody PT9 seems to bind two related epitopes ($_{163}$NATRIPAK$_{174}$ and $_{219}$PTREPK$_{226}$) with a common motif xxTRxP(x)K suggesting the involvement of the positive charge in R/K in the binding. PT9 mAbs showed good binding to PHFs while the Fab showed poor binding to soluble tau suggesting a conformational preference. The exact involvement of both domains in PT9 binding to Tau and PHF tau is not clear, but low binding of PT9 Fab to PHF (data not shown) might exclude a conformational preference of this antibody for PHFs.

Two antibodies bind to the MTBD of Tau; i.e., PT76 and PT83, but their binding epitope in tau is clearly different. PT76 binds to $_{249}$PMPDLKNVKS$_{258}$ which is found in only one of the four repeats while PT83 binds epitopes with xxxPG(G) motif, present in all four repeats of 2N4R tau. C-terminal-targeting hTau21 did show good binding kinetics to both PHF and to 2N4R tau, while PT84 showed strong binding to PHF and weak binding to 2N4R tau. The binding of hTau21 to PHF showed lower RUs suggesting a variable/low abundance of its epitope in PHF. In contrast to tau isoform selectivity (like PT18), the lower signal could be explained by heterogeneous posttranslational modifications (PTM) in the PHFs (e.g., phosphorylation on residue T377) [34] or by a limited exposure of this particular epitope (375–380; Table 1, Supplementary Figure 2B) in the PHF structure. As hTau21 detected both hyperphosphorylated and dephosphorylated tau in the PHF prep under reducing conditions (Supplementary Figure 2C), the phosphorylation at T377 seems relatively rare in PHF or does not affect hTau21 binding. The preference of PT84 for PHF is clearly explained by the requirement of phosphorylation on residue S409 (Table 1, Supplementary Figure 2A) which explains its relative specificity for PHFs observed in the western blots in Fig. 3.

Profiling via western blotting and IHC

Further profiling of antibodies was performed by evaluating their binding to tau in brain samples from different species (mouse, dog, monkey, human). For human tau, a distinction was made between soluble tau (heat-stable extract from non-AD human brain) and aggregated PHF-tau (sarcosyl insoluble prep from human AD brain). To be able to detect lower affinity interactions to non-tau related proteins, antibodies were tested at a concentration of 1 μg/mL and relatively high amounts of brain homogenates (20 μg of total protein) were loaded on the gel. Overview of these profiles is shown in Fig. 3. In addition to western blotting, a selection of antibodies was evaluated by IHC on paraffin sections of WT, Tau KO, and P301S tau transgenic (Tg) mice (age of 6 months with substantial NFT pathology in brainstem, spinal cord, and cortex) [29].

N-terminal antibodies PT26 and PT93 showed binding to monkey and human tau, but not to mouse and dog tau (weak binding by PT93 on tau from dog brain). Additionally, defined non-tau related signals (±20 kDa for PT26 and ± 40 kDa for PT93) were observed in mouse brain homogenate (WT and tau KO) (Fig. 3). IHC data on paraffin sections did not show a signal for PT93 in Tau KO mouse but also not on sections of WT mouse brain. In P301S brain both non-aggregated and aggregated tau were stained (Fig. 4), a similar pattern was observed for PT26 but this antibody displays a non-tau related signal in tau KO sections (data not shown). The isoform-selective isoforms hTau56 and PT18 showed moderate tau binding in the different species, but also non-tau related bands at 100 kDa and 20 kDa, respectively. From the mid-term and PRD-binding antibodies only PT89 showed some non-tau related signals, while the others (PT51, PT79, PT9) were selective for tau with a preference of PT79 for monkey and human Tau. This preference is supported by IHC data (Fig. 4) and suggests a lower sequence homology between murine and human tau in that particular epitope region. Conversely, an antibody with preference for mouse tau, mTau5, binds to a region

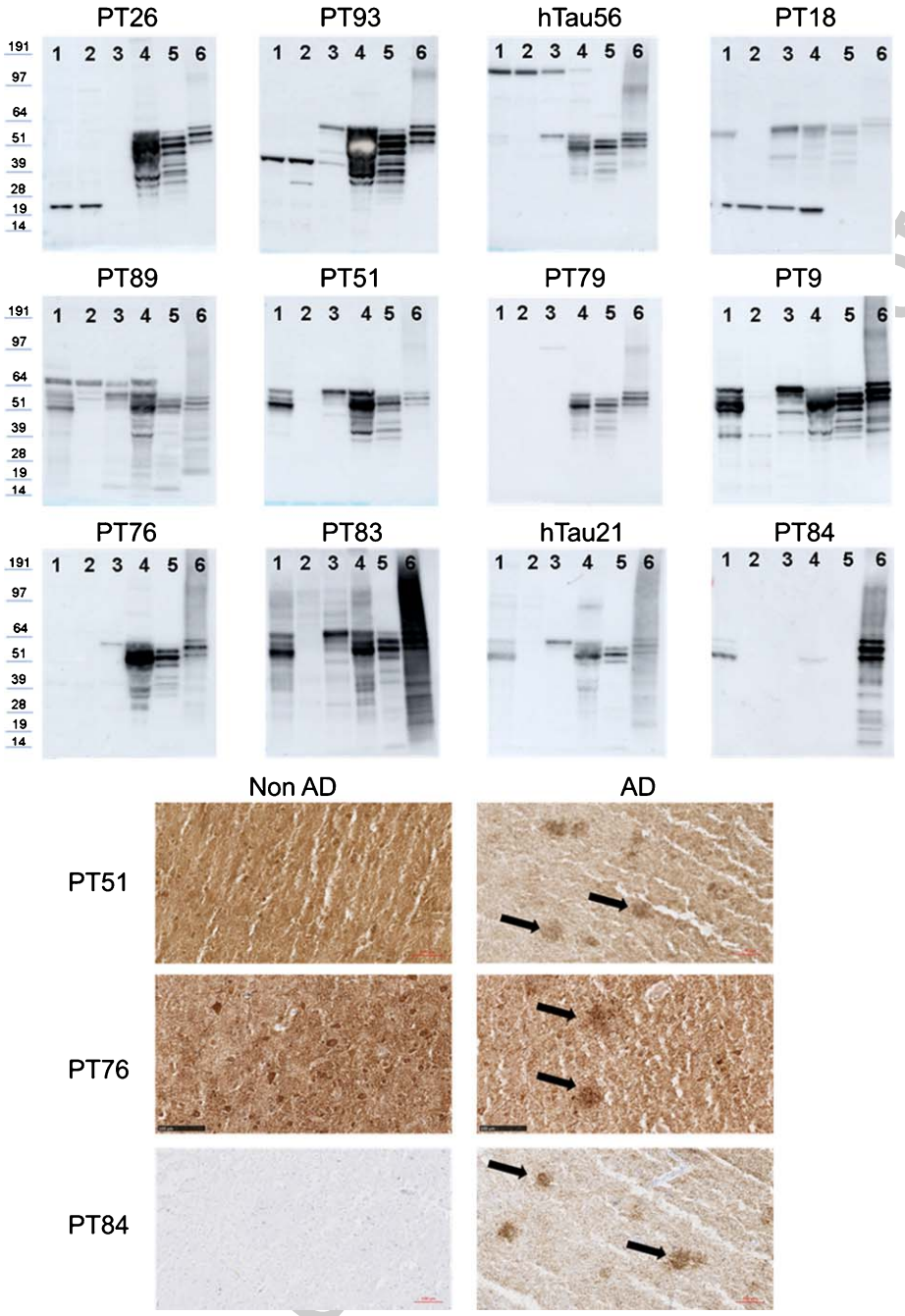

Fig. 3. A) Western blot profiling of indicated anti tau mAbs on brain extracts from WT and tau KO mouse brain, Beagle dog, Cynomolgus monkey, and a heat-stable extract (HSE) from human (non-AD) brain and a PHF prep derived from human AD brain. Sample 1: WT mouse; 2: tau KO; 3: dog; 4: monkey; 5: human HSE; 6: human PHFs. B) IHC profiling on cryosections from human non-AD and AD sections showing a homogeneous staining for total tau antibodies PT51 and PT76 reacting with soluble and aggregated tau (indicated by arrows) and for the phosphorylation selective PT84 antibody showing selectivity for aggregated tau.

in mouse tau corresponding to the PT79 epitope (Table 1).

From the antibodies binding to MTBD, PT76 showed some species preference toward monkey and human tau (Fig. 3) while PT83 showed binding to tau from all species. In addition, weak bands are also observed in brain samples from tau KO mice which could be explained by cross-reactivity with

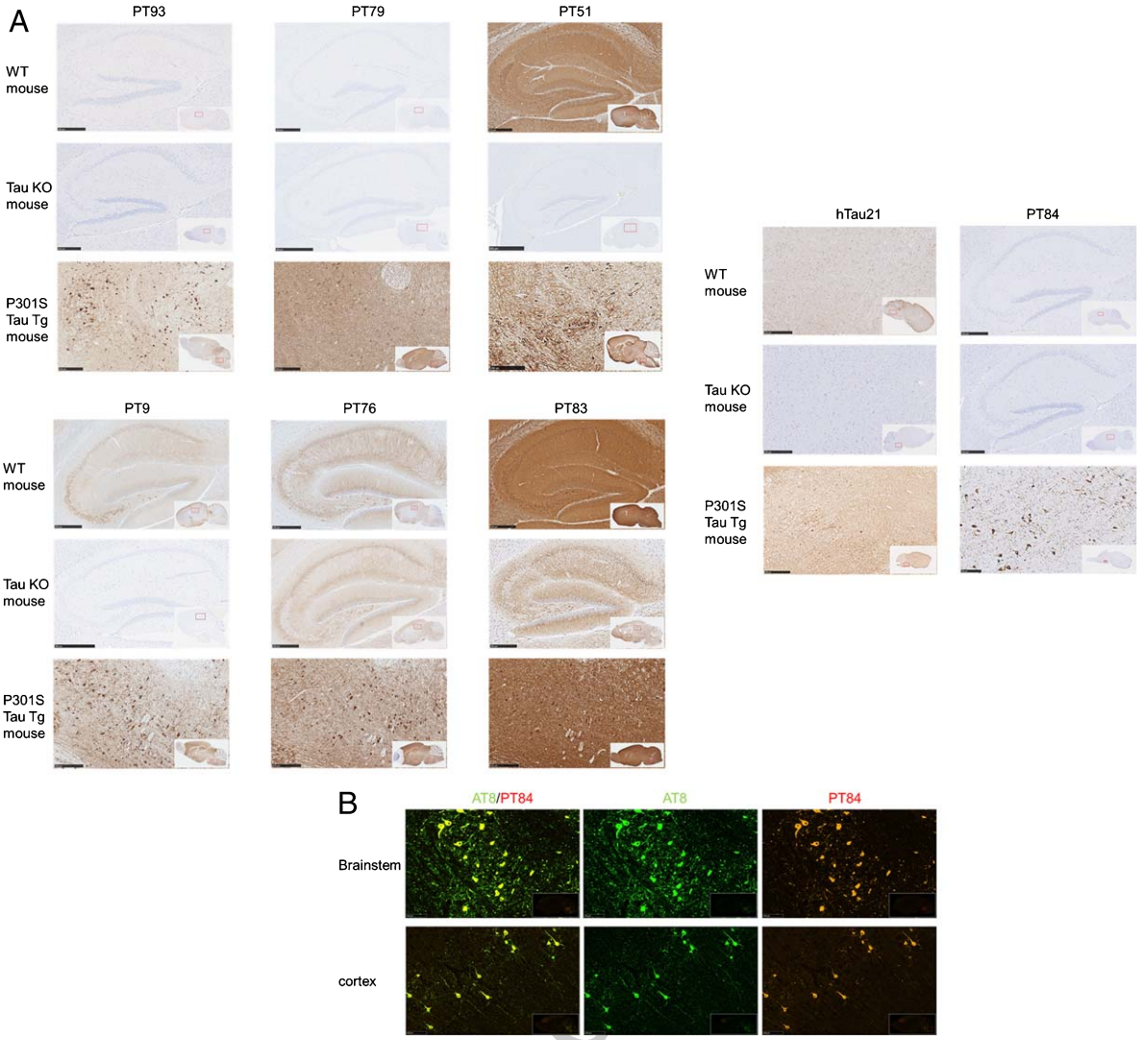

Fig. 4. IHC profiling on a selection of tau mAbs on paraffin sections (A) (saggital) of WT, tau KO and P301S mouse brain and. Selectivity for human tau is observed for N-terminal PT93 and mid-term PT79. Reactivity for both mouse and human tau is observed for PT51, PT9, and hTau21. The axonal staining pattern for PT83 on sections of tau KO mice is explained by its cross-reactivity with other microtubule-associated proteins (e.g., MAP2, MAP4). Double immunofluorescence labelling with AT8 and PT84 on brainstem and cortical sections of P301S tau Tg mice, showed substantial overlap (merge) between the two antibodies and additional staining by AT8 on smaller aggregate species.

other microtubule-associated proteins like MAP2 and/or MAP4. This was also observed in IHC staining (Fig. 4), where PT83 showed high signals in sections from WT and P301S brains but also a somatodendritic staining pattern in Tau KO mice which is similar to a MAP2 pattern (Supplementary Figure 6). As PT76 showed weak binding to mouse tau in western blot (Fig. 3), signals in WT mouse sections are not tau related and are similar to the pattern observed in sections from tau KO mice. The C-terminal antibody hTau21 showed tau binding in all species and in correspondence with the binding data (Table 1) while the pS409-dependent antibody PT84 (Supplementary Figure 2) showed preference for aggregated tau in western blot (Fig. 3A), human cryosections (Fig. 3B), and in sections of P301S mice where partial co-localization with AT8 was observed (Fig. 4A, B).

Functional analysis in a cellular assay

To evaluate the therapeutic potential of the antibodies and/or their binding epitope (region) within the tau molecule, we applied a cell-based seeding assay

using HEK cells expressing two chromophore-tagged tau repeat-domain fragments (K18) that generate a signal if they are in proximity upon aggregation. When the cells are treated with seeds of aggregated and phosphorylated full-size tau derived from different sources, a K18 aggregate is induced that can be quantified by counting fluorescence resonance energy transfer (FRET)-positive cells using fluorescence-activated cell sorting (FACS) [28]. To investigate if the maximum percentage inhibition value is related to the density of epitopes on the seeds or to the number of seeds containing specific epitopes, immunodepletion assays were performed. Two types of seed were used: 1) Tau aggregates isolated from P301S spinal cord homogenate or 2) Total AD brain homogenate. The tau seeds were incubated with test antibody and removed from the solution with protein G beads. The depleted supernatant was tested for residual seeding capacity by adding to the extracellular medium (P301S) or by transfecting into the FRET-cells (human AD seeds) and analyzed by FACS as previously described [28].

From the concentration-response curves outlined in Fig. 5 and Supplementary Figure 3, it can be seen that most antibodies deplete tau seeds from both Tg Tau P301S spinal cord tissue and from human AD brain. Interestingly, N-terminal (PT26, PT93, hTau10) and mid-term antibodies (PT51, PT79, PT89, HT7) showed incomplete depletion of human-derived seeds even at maximal concentration of 300 nM. This concentration seems sufficient for complete depletion of mouse Tg Tau P301S-derived tau seeds, suggesting the presence of tau seeds in AD brain extracts that are not depleted by N-terminal and mid-term antibodies. Even more striking was the lack of effect by hTau21 on human seeds, while a concentration-dependent inhibition was observed on seeds from tau P301S Tg mice. The opposite was observed for MTBD antibodies PT76 and PT83 which both showed complete inhibition at 300 nM. PT76 showed this effect already at 30 nM while seeding by Tg Tau P301S spinal cord homogenate is less potently depleted by PT76. Together with PT9, PT76 seems to be the most efficacious in depleting tau seeds from human AD brain.

Anti-tau antibodies neutralize seeding in vivo

Since immunodepletion experiments showed clear differences between different epitope groups, we wanted to verify whether these differences were translatable to an *in vivo* setting where we evaluated the efficacy of at least one representative antibody for each tau epitope group. Antibodies binding to epitopes that were ineffective in the cellular model, or showing weak binding to human PHFs (e.g., PT18 and hTau56) were not included.

Previously, we demonstrated seeding in P301L mice using *in vitro* aggregated K18 fibrils [23]. Even though this kind of seeds induces a robust pathology, the component responsible for seeding in human brain has different molecular properties and the model is not optimal to evaluate efficacy of tau antibodies with an epitope outside the MTB region. To make this injection model more translational to human tauopathy, we derived PHFs from postmortem human brain by a sarcosyl extraction combined with ultracentrifugation [21]. This type of extraction has been shown to contain seeding competent tau species as described in other studies [18–20] and in Supplementary Figure 4 where high-speed centrifugation pellets contained the largest seeding fractions of P301S tau Tg mouse spinal cord homogenates.

After hippocampal injection, human AD-derived PHFs induced a dose-dependent increase in tau aggregation (mainly in the injected hemisphere), measured by an aggregation selective AT8/AT8 MSD assay (Fig. 6A). In the non-injected hemisphere, AT8 positive deposits are observed as indicated by the red arrows in (Fig. 6A). This model was used to evaluate neutralization of seeding by different anti-tau antibodies. In Fig. 6B, a significant ($p < 0.05$) reduction of 37% is observed by co-injection of PT93 in comparison with a negative control IgG. Also, antibodies binding to the mid-term (PT51 and PT79, Table 2) show incomplete reduction of seeding. In the same model, AT120 and PT76, binding to the tau PRD and MTBD, respectively, exerted a strong inhibition of more than 80% ($p < 0.0001$; Fig. 7B, Table 2). The phosphor-tau selective antibody PT84 showed moderate but significant reduction as well (47% reduction to control, $p < 0.05$) suggesting a lower exposure of this phospho-epitope in human PHFs. In conjunction with the data of the immunodepletion experiments (Fig. 5), it can be concluded that a substantial fraction of human AD seeds is differentially neutralized by N-terminal antibodies and MTBD antibodies and PRD antibodies (AT120, Table 2). The blot in Fig. 6C indeed illustrates the presence of multiple low MW tau species detected by PT76, but not by PT93 suggesting the presence of truncated tau fragments in the PHF prep. Additional western blots (Supplementary Figure 5) confirmed the presence of lower MW tau species in PHF preparations which are detected more

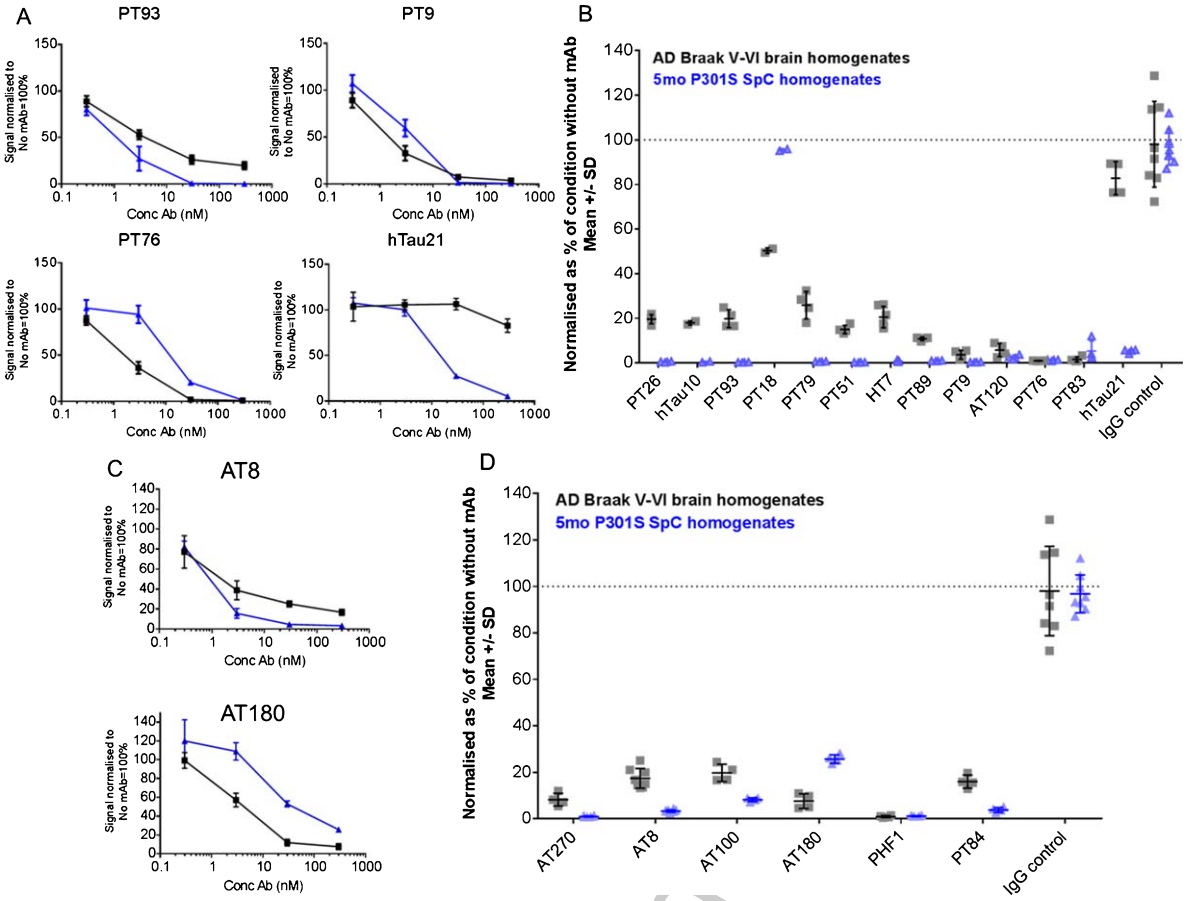

Fig. 5. Concentration-dependent efficacy of the indicated total tau mAbs (A) and phosphorylation sensitive tau mAbs (C) in an immunodepletion assay on human AD brain and P301S spinal cord extracts. Depleted fractions from P301S spinal cord extracts are directly added to the medium and human AD seeds are added by transfection. In both cases, functional analyses were done in a cellular FRET model and are averages ± SD of % remaining seeding signal normalized to the condition without antibody which was taken as 100%. Graphs in panels B and D show maximal efficacy of total- and phosphorylation sensitive antibodies, respectively.

by PRD and MTBD antibodies but not by N-terminal antibodies.

Differences between tau seeds derived from Tg-mice and human AD brain

As N-terminal, mid-term and MTBD antibodies showed differential depletion of tau seeds *in vitro* and *in vivo*, further analysis was conducted to dissect structural differences between these two types of seeds and the relative epitope accessibility.

First, we performed direct ELISA binding experiments to compare binding of a set of antibodies to tau aggregates derived from human AD brain and from P301S tau Tg mice (Fig. 7A). While PT93, hTau10, PT51, and HT7 displayed similar binding curves to both types of tau aggregates, MTBD antibodies PT76 and PT83 show reduced binding to aggregates derived from spinal cord of P301S transgenic mice compared to human AD-brain-derived PHF. To confirm this reduced binding in solution, aggregation-selective MSD assays (PT51-PT51 sulpho-tag; PT76-PT76 sulpho-tag) were set up (Fig. 7B). MSD analysis revealed that PT51 binds equally well to AD PHF and P301S seeds, in opposition to PT76 that only bound efficiently to human PHF. This observation can be explained by a lower affinity of PT76 to P301S seeds or by a lower epitope accessibility on Tau P301S seeds due to a specific structural conformation. Limited proteolysis analysis was also performed and revealed increased epitope exposure for PT76, PT83 (and to a lesser extent for PT51 and hTau21) on P301S seeds after digestion with 5 μg/mL of pronase (Fig. 7C, green box), which was not observed for AD PHF samples. This supported the hypothesis that the conformation of tau aggregates in Tau

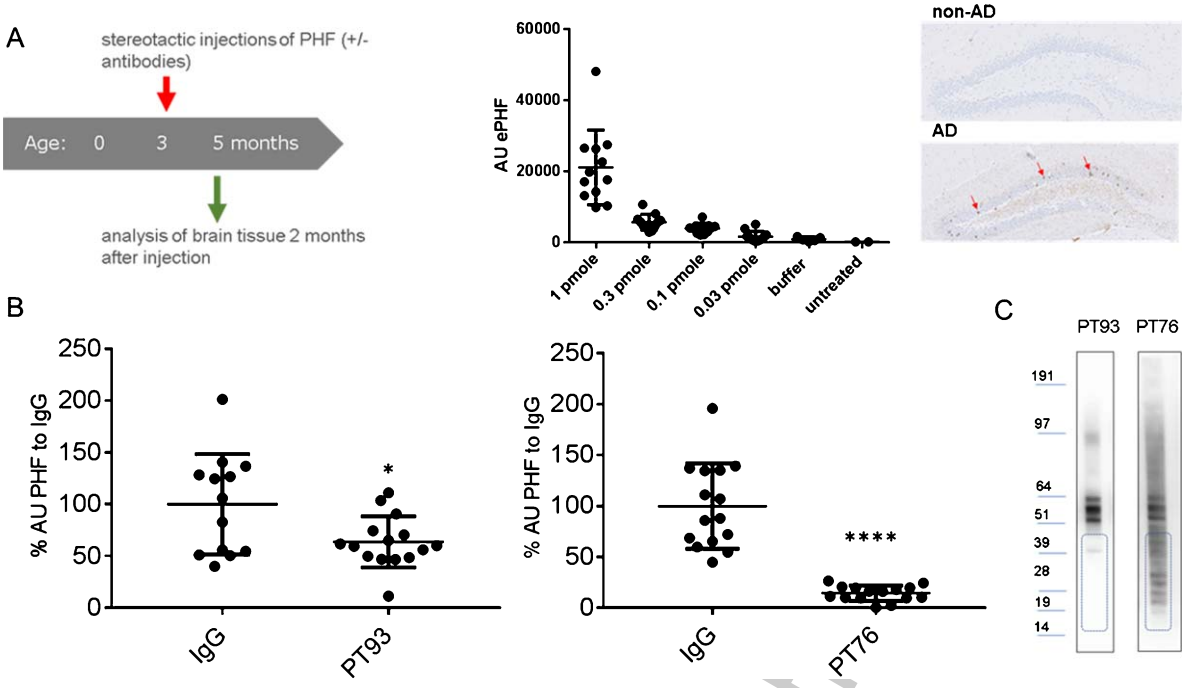

Fig. 6. Efficacy of the indicated tau mAbs in an *in vivo* co-injection model. A) Human AD brain-derived PHFs (increasing amounts as indicated in the graph) are injected in the right hippocampus of 3-month-old P301L mice. Two months after injection (at an age of 5 months), mice are sacrificed and brain homogenates are analyzed with AT8/AT8 aggregation selective MSD assay showing a dose-dependent increase in tau aggregation. IHC staining of the contralateral hemisphere showed a modest but significant number of neurons with AT8-positive deposits (red arrows) for the 1 pmole ePHF dose. This model was used to evaluate efficacy of different tau antibodies upon co-injection with PHFs. B) Co-injection of PHFs with the indicated tau antibodies reduced the induction of tau pathology. From the internal N-terminal antibodies and MTBD binding antibodies a representative example (PT93 and PT76 respectively) is shown. (*$p<0.05$; ****$p<0.0001$, student T-test). C) Representative profiles of a PHF sample analyzed by western blotting using PT93 and PT76. A clear difference in pattern was observed in the lower MW region indicated by blue rectangles suggesting the presence of truncated tau fragments in the PHFs.

P301S seeds interfere with the binding of PT76. Conversely, increased pronase concentration resulted in the formation of smaller proteolytic-resistant fragments forming the core of the fibrils (Fig. 7C, purple box for AD PHF and red box for P301S aggregates). While PT76 stained the pronase-resistant fragments more efficiently in P301S-derived seeds, PT83 showed similar detection and hTau21 displayed a more intense signal of these fragments from human-derived PHFs. It should be noted that the pattern of bands obtained in AD PHF and mice seeds differed after digestion with enzyme and that detection with N-terminal antibodies (hTau10, PT93) and mid-term (PT51) resulted in no signal for the digested samples. Our findings were consistent with studies using cryo-EM showing that the N-terminal sequence of tau is part of the "fuzzy-coat" which probably makes this terminal more exposed to enzymatic degradation and that the epitopes of PT76, PT83 and hTau21 antibodies are close or within in the proteolytic resistant core of the tau filaments [35]. Their differential staining towards pronase-resistant fragments on human- and Tg mice filaments suggests a different exposure of their epitopes on both type of tau seeds.

DISCUSSION

The tau spreading hypothesis provides rationale for passive immunization with an anti-tau monoclonal antibody to block seeding by extracellular tau aggregates as a disease-modifying strategy for the treatment of AD and potentially other tauopathies. Several studies have demonstrated antibody efficacy in transgenic mouse models [15, 16] but, despite the variety of research models, the species of tau responsible for the tauopathy spread is elusive. In a study with low-molecular weight aggregates, short fibrils or long fibrils of recombinant full-length tau, only aggregates and short fibrils were internalized. Furthermore, HEK cells overexpressing a monomeric or oligomeric recombinant tau microtubule-binding domain (amino acids 243 to 375) (K18) formed

Table 2
Overview of antibody efficacy studies in a PHF-injection model

Antibody	Epitope	% inhibition in co-injection model	*p*-value
PT93	$_{27}$YTMHQD$_{32}$	36	0.0175
PT51	$_{153}$TPRGAA$_{158}$	47	0.012
PT79	$_{131}$(SK)DGTGSDDKK$_{140}$	34	0.09
AT120	$_{219}$PTREPK$_{226}$	82	<0.0001
PT76	$_{249}$PMPDLKNVKS$_{258}$	85	<0.0001
PT84	$_{405}$PRHLpSN$_{410}$	47	0.0367

Human AD brain-derived PHFs (increasing amounts as indicated in the graph) are injected in the right hippocampus of 3-month-old P301L mice. Two months after injection (at an age of 5 months), mice are sacrificed and brain homogenates are analyzed with AT8/AT8 aggregation selective MSD. Values in the table represent % inhibition compared to the mice injected with PHF and control IgG2a antibody.

aggregates which were released and internalized by other HEK cells, suggesting that these fragments can be transferred between cells *in vitro* [36]. In addition, the type of seed that is added to the cells determines the properties of the aggregates supporting the conformational templating hypothesis [31]. More recently it has been suggested that in this model, a clear minimum size (monomeric-trimeric tau) exists for spontaneous propagation of tau aggregation from the outside to the inside of the cell [37], whereas many larger sizes of soluble aggregates trigger uptake and seeding (Supplementary Figure 4) [18, 20]. *In vivo* injection studies confirmed seeding potential of K18 (P301L)-derived fibrils. The fact that sonication of these fibrils is needed suggests that smaller or short fibrils are needed for seeding [23, 38]. In addition, fibrils prepared from tau transgenic mouse- and human AD brain recapitulate tau seeding *in vivo* [15, 19, 20], which is also confirmed by internal studies (Fig. 6A). Therefore, PHF tau was considered as a promising antigen for our immunization strategy to generate anti-tau antibodies for therapeutic and research purposes. Other immunizations were performed with soluble tau and *in vitro* aggregated tau (Fig. 1A, B).

In this communication, we report on several in-house produced antibodies obtained by these different immunization campaigns (Fig. 1A, B). From each domain (N-terminus (PT26, PT93), mid-term (PT51, PT79, PT89), PRD (PT9), MTBD (PT76, PT83) and C-terminus (hTau21, PT84)) at least one

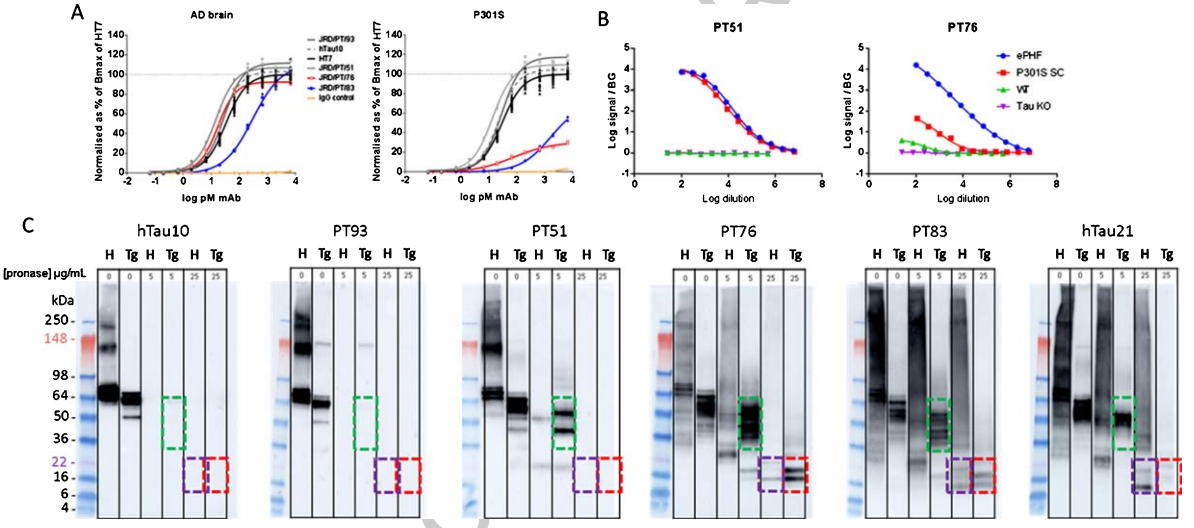

Fig. 7. Biochemical comparison between tau seeds from P301S mice and from human AD brain. A) Direct ELISA binding curves of PT93, hTau10, PT51, HT7, PT76, and PT83 to tau aggregates from human brain or spinal cord from P301S tau Tg mouse as indicated. To allow comparing curves from different ELISA plates, signals are normalized to the Bmax value of HT7 (=100%) which was taken along as a reference curve on all plates. Data are average ± SD of at least 2 independent experiments. B) Tau aggregation-selective MSD assays were developed by capturing and detection with the same antibody, ruling out detection of monomeric tau. Representative dilution curves of AD PHFs and P301S tau Tg mouse filaments were analyzed with PT51/PT51 and PT76/PT76 MSD assays showing almost no signal in homogenates from WT and tau KO mouse brain. PT51/PT51 displayed similar sensitivity toward both aggregate species while PT76/PT76 showed weaker reactivity toward aggregates from tau Tg mice. To evaluate epitope exposure of N-terminal, mid-term, MTBD and more C-terminal antibodies, limited proteolysis reactions of human AD PHF (H) and P301S tau Tg mouse (Tg) filaments were performed with 0, 5, or 25 µg/mL of enzyme as indicated. C) Samples were analyzed by western blotting with the indicated antibodies. Green rectangle reflects increased exposure of epitopes (in particular PT76 and PT83) under condition of incomplete proteolysis. Proteolytic resistant fragments from AD PHF and P301S tau filaments are indicated by purple and red rectangles, respectively.

antibody is represented including isoform specific antibodies to 1N- and 2N- domains (hTau56 and PT18, respectively). In general, N- and mid-term antibodies showed more selectivity for human tau (Figs. 3 and 4) but showed cross reactivity to tau from monkey brain. In the other epitope regions sequences are better conserved, and hence more cross reactivity is observed (e.g., PT9, hTau21). In addition, some non-tau related signals were observed. Some of these were not expected and were not observed in brain sections from Tau KO mice (PT26, PT93, PT89), while non-tau reactivity of MTBD (weak detection on western blot; somatodendritic staining in Tau KO sections) antibodies PT76 and PT83 was expected.

Looking at the functional properties of the different antibodies, some differences are observed between the different epitopes:

(1) Sub-maximal effect in immunodepletion of human AD seeds by N- and mid-term antibodies in comparison to PRD- and MTBD antibodies (Fig. 5) which is also confirmed in an *in vivo* co-injection experiment (Fig. 6; Table 2). Since recent high resolution cryo-EM studies on human AD PHFs suggested exposure of the N-terminal domain, confirming that the N-terminus is part of the "fuzzy coat", our results seem to be counterintuitive. On the other hand, extensive hydrolysis at the N-terminus could result in a reduced epitope density on a number of PHF seeds [39]. Indeed, comparison of PT93 and PT76 western blots profiles of a human PHF extract showed multiple lower MW bands detected by PT76 that are not detected by PT93 and other N-terminal antibodies (Fig. 6C, Supplementary Figure 5), suggesting more processing at the N-terminus on PHF seeds. The latter phenomenon is not observed with seeds derived from tau transgenic mouse extracts.

(2) A number of antibodies displayed differential activity toward AD brain-derived seeds and seeds derived from tau Tg mice (Fig. 5). PT76, which binds to the MTB region in tau, efficiently depleted human seeds, but was less potent in reducing seeding by spinal cord extracts of tau P301S Tg mice (Fig. 5A, B) and PT83, which binds to all four repeats, showed low potency (but strong inhibition at 300 nM) to both types of seeds (Fig. 5B, Supplementary Figure 3). Recent data demonstrated that in tau filaments the MTBD is not accessible for proteolytic enzymes excluding the possibility of a truncated epitope [40]. Therefore, the difference in efficacy of both PT76 and PT83 toward PHFs in human AD and straight filaments in transgenic mouse brain is explained by structural differences between both types of tau aggregates [29, 35, 40]. This is further supported by the differential depletion of human AD- and P301S tau Tg mouse-derived seeds by hTau21 (Fig. 5A) which is not explained by truncation as high efficacy of the more C-terminal phospho-selective PHF1 antibodies (Fig. 5D) rules out a loss of binding epitopes due to hydrolysis [39]. Although the epitope of PT84 is also C-terminal, its immunodepletion activity toward human AD seeds was less prominent compared to PHF1 suggesting that phosphorylation at S409 is less common in human PHFs. The moderate (but significant) reduction by this antibody *in vivo* (Table 2). Limited proteolysis experiments demonstrated a pronase-resistant core which is detected by PT83 in filaments from human AD brain and from P301S tau Tg mice. Interestingly, PT76 showed lower staining in the core of human tau filaments and stronger signal in the mutant mouse filaments while hTau21 displayed the opposite profile suggesting that epitopes from these antibodies are differentially exposed in both types of filaments [35].

In conclusion, we describe a panel of antibodies with diverse properties with respect to their epitope location and sensitivity to post translational modifications. Some of these antibodies show different neutralization efficacy towards tau seeds from AD brain and from transgenic mouse models demonstrating that potency toward tau filaments from mouse models does not immediately translate into the desired effect on human AD tau seeds. In addition, the therapeutic potential of tau antibodies is currently under clinical evaluation [41], but functional data highlight differences in efficacy by different epitope binding on human AD seeds suggesting that not all epitopes are optimal targets for immunotherapy to block tau spreading.

ACKNOWLEDGMENTS

Human brain tissue for the immunodepletion experiments performed in this study was provided by the Newcastle Brain Tissue Resource which is

funded in part by a grant from the UK Medical Research Council (G0400074), by NIHR Newcastle Biomedical Research Centre and Unit awarded to the Newcastle upon Tyne NHS Foundation Trust and Newcastle University, and as part of the Brains for Dementia Research Programme jointly funded by Alzheimer's Research UK and Alzheimer's Society.

The authors wish the thank Drs. Steven Paul and Wencheng Liu (Weill Medical College of Cornell University, New York, USA) for kindly providing the PHF material for immunization of mice. We thank Werner Schillebeeckx and Nicole Kersemans for their excellent assistance during the *in vivo* experiments. Discussions with Dr. Jaap-Willem Back and Dr. Ekaterina Shimanovskaya (Pepscan Presto, the Netherlands) on epitope mapping analysis was highly appreciated. Support was provided by VLAIO (AD immunotherapy project 150882) and A.M. received funding from VLAIO (Baekeland project 140773).

Authors' disclosures available online (https://www.j-alz.com/manuscript-disclosures/18-0404r1).

SUPPLEMENTARY MATERIAL

The supplementary material is available in the electronic version of this article: http://dx.doi.org/10.3233/JAD-180404.

REFERENCES

[1] Chiti F, Dobson CM (2006) Protein misfolding, functional amyloid, and human disease. *Annu Rev Biochem* **75**, 333-366.

[2] Lee VM, Goedert M, Trojanowski JQ (2001) Neurodegenerative tauopathies. *Annu Rev Neurosci* **24**, 1121-1159.

[3] Spillantini MG, Goedert M (2013) Tau pathology and neurodegeneration. *Lancet Neurol* **12**, 609-622.

[4] Binder LI, Frankfurter A, Rebhun LI (1985) The distribution of tau in the mammalian central nervous system. *J Cell Biol* **101**, 1371-1378.

[5] Wolfe MS (2009) Tau mutations in neurodegenerative diseases. *J Biol Chem* **284**, 6021-6025.

[6] Lasagna-Reeves CA, Castillo-Carranza DL, Jackson GR, Kayed R (2011) Tau oligomers as potential targets for immunotherapy for Alzheimer's disease and tauopathies. *Curr Alzheimer Res* **8**, 659-665.

[7] Lasagna-Reeves CA, Castillo-Carranza DL, Sengupta U, Guerrero-Munoz MJ, Kiritoshi T, Neugebauer V, Jackson GR, Kayed R (2012) Alzheimer brain-derived tau oligomers propagate pathology from endogenous tau. *Sci Rep* **2**, 700.

[8] Lasagna-Reeves CA, Castillo-Carranza DL, Sengupta U, Sarmiento J, Troncoso J, Jackson GR, Kayed R (2012) Identification of oligomers at early stages of tau aggregation in Alzheimer's disease. *FASEB J* **26**, 1946-1959.

[9] Braak H, Braak E (1991) Neuropathological stageing of Alzheimer-related changes. *Acta Neuropathol* **82**, 239-259.

[10] Braak H, Thal DR, Ghebremedhin E, Del TK (2011) Stages of the pathologic process in Alzheimer disease: Age categories from 1 to 100 years. *J Neuropathol Exp Neurol* **70**, 960-969.

[11] Goedert M, Falcon B, Clavaguera F, Tolnay M (2014) Prion-like mechanisms in the pathogenesis of tauopathies and synucleinopathies. *Curr Neurol Neurosci Rep* **14**, 495.

[12] Calafate S, Buist A, Miskiewicz K, Vijayan V, Daneels G, de SB, de WJ, Verstreken P, Moechars D (2015) Synaptic contacts enhance cell-to-cell tau pathology propagation. *Cell Rep* **11**, 1176-1183.

[13] Clavaguera F, Hench J, Goedert M, Tolnay M (2015) Invited review: Prion-like transmission and spreading of tau pathology. *Neuropathol Appl Neurobiol* **41**, 47-58.

[14] de Calignon A, Polydoro M, Suarez-Calvet M, William C, Adamowicz DH, Kopeikina KJ, Pitstick R, Sahara N, Ashe KH, Carlson GA, Spires-Jones TL, Hyman BT (2012) Propagation of tau pathology in a model of early Alzheimer's disease. *Neuron* **73**, 685-697.

[15] Chai X, Wu S, Murray TK, Kinley R, Cella CV, Sims H, Buckner N, Hanmer J, Davies P, O'Neill MJ, Hutton ML, Citron M (2011) Passive immunization with anti-Tau antibodies in two transgenic models: Reduction of Tau pathology and delay of disease progression. *J Biol Chem* **286**, 34457-34467.

[16] Yanamandra K, Kfoury N, Jiang H, Mahan TE, Ma S, Maloney SE, Wozniak DF, Diamond MI, Holtzman DM (2013) Anti-tau antibodies that block tau aggregate seeding *in vitro* markedly decrease pathology and improve cognition *in vivo*. *Neuron* **80**, 402-414.

[17] Theunis C, Crespo-Biel N, Gafner V, Pihlgren M, Lopez-Deber MP, Reis P, Hickman DT, Adolfsson O, Chuard N, Ndao DM, Borghgraef P, Devijver H, Van LF, Pfeifer A, Muhs A (2013) Efficacy and safety of a liposome-based vaccine against protein Tau, assessed in tau.P301L mice that model tauopathy. *PLoS One* **8**, e72301.

[18] Audouard E, Houben S, Masaracchia C, Yilmaz Z, Suain V, Authelet M, De DR, Buee L, Boom A, Leroy K, Ando K, Brion JP (2016) High-molecular-weight paired helical filaments from Alzheimer brain induces seeding of wild-type mouse tau into an argyrophilic 4R tau pathology *in vivo*. *Am J Pathol* **186**, 2709-2722.

[19] Guo JL, Narasimhan S, Changolkar L, He Z, Stieber A, Zhang B, Gathagan RJ, Iba M, McBride JD, Trojanowski JQ, Lee VM (2016) Unique pathological tau conformers from Alzheimer's brains transmit tau pathology in nontransgenic mice. *J Exp Med* **213**, 2635-2654.

[20] Jackson SJ, Kerridge C, Cooper J, Cavallini A, Falcon B, Cella CV, Landi A, Szekeres PG, Murray TK, Ahmed Z, Goedert M, Hutton M, O'Neill MJ, Bose S (2016) Short fibrils constitute the major species of seed-competent tau in the brains of mice transgenic for human P301S tau. *J Neurosci* **36**, 762-772.

[21] Greenberg SG, Davies P (1990) A preparation of Alzheimer paired helical filaments that displays distinct tau proteins by polyacrylamide gel electrophoresis. *Proc Natl Acad Sci U S A* **87**, 5827-5831.

[22] Malia TJ, Teplyakov A, Ernst R, Wu SJ, Lacy ER, Liu X, Vandermeeren M, Mercken M, Luo J, Sweet RW, Gilliland GL (2016) Epitope mapping and structural basis for the recognition of phosphorylated tau by the anti-tau antibody AT8. *Proteins* **84**, 427-434.

[23] Peeraer E, Bottelbergs A, Van KK, Stancu IC, Vasconcelos B, Mahieu M, Duytschaever H, Ver DL, Torremans A, Sluydts E, Van AN, Kemp JA, Mercken M, Brunden KR,

Trojanowski JQ, Dewachter I, Lee VM, Moechars D (2015) Intracerebral injection of preformed synthetic tau fibrils initiates widespread tauopathy and neuronal loss in the brains of tau transgenic mice. *Neurobiol Dis* **73**, 83-95.

[24] Kohler G, Milstein C (1975) Continuous cultures of fused cells secreting antibody of predefined specificity. *Nature* **256**, 495-497.

[25] Timmerman P, Puijk WC, Meloen RH (2007) Functional reconstruction and synthetic mimicry of a conformational epitope using CLIPS technology. *J Mol Recognit* **20**, 283-299.

[26] Vandermeeren M, Mercken M, Vanmechelen E, Six J, van d, V, Martin JJ, Cras P (1993) Detection of tau proteins in normal and Alzheimer's disease cerebrospinal fluid with a sensitive sandwich enzyme-linked immunosorbent assay. *J Neurochem* **61**, 1828-1834.

[27] Goedert M, Jakes R, Crowther RA, Cohen P, Vanmechelen E, Vandermeeren M, Cras P (1994) Epitope mapping of monoclonal antibodies to the paired helical filaments of Alzheimer's disease: Identification of phosphorylation sites in tau protein. *Biochem J* **301**(Pt 3), 871-877.

[28] Holmes BB, Furman JL, Mahan TE, Yamasaki TR, Mirbaha H, Eades WC, Belaygorod L, Cairns NJ, Holtzman DM, Diamond MI (2014) Proteopathic tau seeding predicts tauopathy *in vivo*. *Proc Natl Acad Sci U S A* **111**, E4376-E4385.

[29] Allen B, Ingram E, Takao M, Smith MJ, Jakes R, Virdee K, Yoshida H, Holzer M, Craxton M, Emson PC, Atzori C, Migheli A, Crowther RA, Ghetti B, Spillantini MG, Goedert M (2002) Abundant tau filaments and nonapoptotic neurodegeneration in transgenic mice expressing human P301S tau protein. *J Neurosci* **22**, 9340-9351.

[30] Terwel D, Lasrado R, Snauwaert J, Vandeweert E, Van HC, Borghgraef P, Van LF (2005) Changed conformation of mutant Tau-P301L underlies the moribund tauopathy, absent in progressive, nonlethal axonopathy of Tau-4R/2N transgenic mice. *J Biol Chem* **280**, 3963-3973.

[31] Sanders DW, Kaufman SK, DeVos SL, Sharma AM, Mirbaha H, Li A, Barker SJ, Foley AC, Thorpe JR, Serpell LC, Miller TM, Grinberg LT, Seeley WW, Diamond MI (2014) Distinct tau prion strains propagate in cells and mice and define different tauopathies. *Neuron* **82**, 1271-1288.

[32] Greenberg SG, Davies P, Schein JD, Binder LI (1992) Hydrofluoric acid-treated tau PHF proteins display the same biochemical properties as normal tau. *J Biol Chem* **267**, 564-569.

[33] Lee VM, Goedert M, Trojanowski JQ (2001) Neurodegenerative tauopathies. *Annu Rev Neurosci* **24**, 1121-1159.

[34] Amano M, Kaneko T, Maeda A, Nakayama M, Ito M, Yamauchi T, Goto H, Fukata Y, Oshiro N, Shinohara A, Iwamatsu A, Kaibuchi K (2003) Identification of Tau and MAP2 as novel substrates of Rho-kinase and myosin phosphatase. *J Neurochem* **87**, 780-790.

[35] Fitzpatrick AWP, Falcon B, He S, Murzin AG, Murshudov G, Garringer HJ, Crowther RA, Ghetti B, Goedert M, Scheres SHW (2017) Cryo-EM structures of tau filaments from Alzheimer's disease. *Nature* **547**, 185-190.

[36] Kfoury N, Holmes BB, Jiang H, Holtzman DM, Diamond MI (2012) Trans-cellular propagation of Tau aggregation by fibrillar species. *J Biol Chem* **287**, 19440-19451.

[37] Mirbaha H, Holmes BB, Sanders DW, Bieschke J, Diamond MI (2015) Tau trimers are the minimal propagation unit spontaneously internalized to seed intracellular aggregation. *J Biol Chem* **290**, 14893-14903.

[38] Iba M, Guo JL, McBride JD, Zhang B, Trojanowski JQ, Lee VM (2013) Synthetic tau fibrils mediate transmission of neurofibrillary tangles in a transgenic mouse model of Alzheimer's-like tauopathy. *J Neurosci* **33**, 1024-1037.

[39] Endoh R, Ogawara M, Iwatsubo T, Nakano I, Mori H (1993) Lack of the carboxyl terminal sequence of tau in ghost tangles of Alzheimer's disease. *Brain Res* **601**, 164-172.

[40] Taniguchi-Watanabe S, Arai T, Kametani F, Nonaka T, Masuda-Suzukake M, Tarutani A, Murayama S, Saito Y, Arima K, Yoshida M, Akiyama H, Robinson A, Mann DMA, Iwatsubo T, Hasegawa M (2016) Biochemical classification of tauopathies by immunoblot, protein sequence and mass spectrometric analyses of sarkosyl-insoluble and trypsin-resistant tau. *Acta Neuropathol* **131**, 267-280.

[41] Panza F, Solfrizzi V, Seripa D, Imbimbo BP, Lozupone M, Santamato A, Tortelli R, Galizia I, Prete C, Daniele A, Pilotto A, Greco A, Logroscino G (2016) Tau-based therapeutics for Alzheimer's disease: Active and passive immunotherapy. *Immunotherapy* **8**, 1119-1134.